Acidic Porous Clay Heterostructures (PCH): Intragallery Assembly of Mesoporous Silica in Synthetic Saponite Clays

Mihai Polverejan, Thomas R. Pauly, and Thomas J. Pinnavaia*

Department of Chemistry, Michigan State University, East Lansing, Michigan 48824

Received March 27, 2000. Revised Manuscript Received June 7, 2000

Mesostructured intercalates belonging to the class of solid acids known as porous clay heterostructures (PCH) have been prepared through the surfactant-directed assembly of mesoporous silica within the galleries of synthetic saponite clays with targeted layer charge densities in the range $x = 1.2-1.7$ e^- units per $Q^+_x[Mg_6](Si_{8-x}Al_x)O_{20}(OH)_4$ unit cell. The removal of the intragallery mixture of neutral alkylamine and quaternary ammonium ion surfactant (Q^+) by calcination afforded PCH intercalates with basal spacings of 33−35 Å, BET specific surface areas of 800−920 $m^2\ g^{-1}$, and pore volumes of 0.38−0.44 $cm^3\ g^{-1}$. The framework pore sizes were in the supermicropore to small mesopore region ∼15−23 Å. Temperature-programmed desorption of chemisorbed cyclohexylamine (CHA) indicated the presence of both weak and strong acid sites, corresponding to desorption temperatures near 220 and 410 °C, respectively. The total acidity (0.64−0.77 mmol CHA g^{-1}) increased with the saponite layer charge density (x), indicating that the acidity is correlated with the number of protons balancing the clay layer charge after calcination. The high acidity, structural stability to 750 °C, and supermicroporous to small mesoporous pore structure of these intermediates make these PCH materials especially attractive candidates for acid-catalyzed conversions of organic molecules.

Introduction

Environmental concerns have raised a great deal of interest in the substitution of traditional acid catalysts such as aluminum chloride and sulfuric and hydrofluoric acids with solid-state alternatives, particularly microporous pillared clays[1−3] and mesoporous molecular sieves.[4−8] We recently reported the discovery of yet a third class of solid porous materials known as porous clay heterostructures[9] (denoted PCH) that showed promising acidic properties for catalytic organic conversions.[10,11] These materials were prepared by the surfactant-directed assembly of mesostructured silica in the two-dimensional galleries of 2:1 mica-type layered silicate with high charge density, such as in fluorohectorite, rectorite, and vermiculite.

In general, PCH materials offer special opportunities for the rational design of a heterogeneous catalyst system, in part, because the pore size distribution can be tailored in the rarely encountered supermicropore to small mesopore range (14−25 Å) through the choice of the structure-directing surfactant in the galleries. However, the choice of a host clay with a charge density suitable for the intragallery assembly is somewhat problematic. Although vermiculite occurs abundantly in nature, this mineral is almost always contaminated with iron impurities that can compromise catalytic properties. Rectorite, although found abundantly in China, is not commercially available. Neither mineral is easily synthesized. Fluorohectorite, on the other hand, can be easily synthesized from molten fluxes, but PCH derivatives based on fluorohectorite are thermally unstable and undergo defluorination above 350 °C. Therefore, more readily accessible synthetic smectite clays with high layer charge density are needed to fully develop the chemistry of PCH materials.

Here we report the synthesis and properties of a new family of porous clay heterostructures derived from synthetic saponite clay. In this smectic clay, the layer charge density can be regulated by controlling the extent of silicon substitution by aluminum in the tetrahedral sheet of the 2:1 layer. Also, saponite can be synthesized[12] free of impurities from readily accessible starting materials under hydrothermal conditions. Moreover, intercalated derivatives of saponite are intrinsically

* E-mail address: pinnavaia@cem.msu.edu.

(1) Figueras, F. *Catal. Rev.-Sci. Eng.* **1998**, *30*, 457.
(2) Izumi, Y.; Urabe, K.; Onaka, M. *Zeolites, Clay and Heteropoly Acid in Organic Reactions*; VCH Publishers: New York, 1992; p 49.
(3) Butruille, J.-R.; Pinnavaia, T. J. *Catal. Today* **1992**, *14*, 141.
(4) Kresge, C. T.; Leonowicz, M. E.; Roth, W. J.; Vartuli, J. C.; Beck, J. S. *Nature* **1992**, *359*, 710.
(5) Huo, Q.; Margolese, D. I.; Ciesla, U.; Feng, P.; Gier, T. E.; Sieger, P.; Leon, R.; Petroff, P. M.; Schuth, F.; Stucky, G. D. *Nature* **1994**, *368*, 317.
(6) Raman, N. K.; Anderson, M. T.; Brinker, C. J. *Chem. Mater.* **1996**, *8*, 1682.
(7) Corma, A. *Chem. Rev.* **1997**, *97*, 2373.
(8) Sayari, A. *Chem. Mater.* **1996**, *8*, 1840.
(9) Galarneau, A.; Barodawalla, A.; Pinnavaia, T. J. *Nature* **1995**, *374*, 529.
(10) Galarneau, A.; Barodawalla, A.; Pinnavaia, T. J. *Chem. Commun.* **1997**, 1661.
(11) Galarneau, A.; Barodawalla, A.; Pinnavaia, T. J. Proc. 11th Int. Clay Conf., Ottawa, Canada, 1997, 21.
(12) Vogels, R. J. M. J.; Breukelaar, J.; Kloprogge, J. T.; Jansen, J. B. H.; Geus, J. W. *Clays Clay Miner.* **1997**, *45*, 1.

10.1021/cm0002618 CCC: $19.00
Published on Web 08/23/2000

acidic, as has been demonstrated previously for alumina pillared forms of the mineral.[13−15]

Experimental Section

Saponite Synthesis. Synthetic saponites were prepared by the hydrothermal crystallization of gels (Si/Al = 5.67−3.57) in the temperature range 175−200 °C following the general methodology reported by Vogels et al.[12] The as-synthesized products were thoroughly washed with deionized water, filtered, and dried overnight in an oven at 120 °C.

PCH Synthesis. Cetyltrimethylammonium (CTMA) as the clay exchange cation and decylamine as the cosurfactant were used to form the PCH forms of the synthetic saponites. A 1.0 wt % suspension of previously prepared saponite was allowed to react at 50 °C with a 0.5 M aqueous cetyltrimethylammonium bromide solution in 2-fold excess of the clay cation exchange capacity. After a reaction time of 24 h, the product was washed with ethanol and water to remove excess surfactant and air-dried. The organoclay, denoted Q^+-clay, was then added to decylamine at a Q^+-clay:decylamine molar ratio of 1:20 and the resulting suspension was stirred for 20 min at room temperature. The amine cosurfactant swells the galleries and participates in the gallery assembly process. Tetraethyl orthosilicate (TEOS) was added to achieve the molar ratio decylamine:TEOS = 1:6. After a reaction time of 3 h at room temperature the gel was recovered by centrifugation and exposed to a controlled relative humidity of 50% for a period of 72 h to form the as-synthesized product. The resulting white powder was subsequently calcined in air at 650 °C using a temperature ramp rate of 1 °C/min to remove the surfactant.

All reactants were obtained from Aldrich Chemical Co. and used without further purification.

Physical Measurements. The cation exchange capacity (CEC) of the saponite was determined from the ammonium content in solution after exchange with NaOH using an ammonia selective electrode.

Elemental analyses were carried out by inductively coupled plasma emission spectroscopy at the University of Illinois Elemental Analysis Laboratory.

Powder X-ray diffraction patterns were obtained on a Rigaku Rotaflex diffractometer equipped with a rotating anode (Cu Kα radiation) operated at 45 kV and 100 mA. The scattering and receiving slits were $^1/_6$° and 0.3°, respectively.

^{29}Si MAS (magic angle spinning) NMR spectra were obtained on a Varian VXR 400 MHz spectrometer at 79.5 MHz using a 7 mm zirconia rotor and a sample spinning frequency of 4 kHz. A pulse duration of 9 μs and a delay time of 600 s allowed for a full relaxation of the Si nucleus. An external reference of talc ($\delta = -98.1$ ppm relative to TMS) was used to determine the chemical shift values.

N_2 adsorption−desorption isotherms were obtained at −196 °C on a Micromeritics ASAP 2010 Sorptometer using static adsorption procedures. Samples were outgassed at 175 °C and 10^{-6} Torr for a minimum of 12 h prior to analysis. BET specific surface areas were calculated from the linear part of the BET plot according to IUPAC[16] recommendations.

TEM images were obtained on a JEOL JEM-100CX II microscope with a CeB_6 filament and an accelerating voltage of 120 kV, a beam diameter of ~5 μm and an objective lens aperture of 20 μm. TEM samples were prepared either by sonication of the powder in ethanol for 20 min and evaporating 1 drop onto a holey carbon film or by thin sectioning. Thin sections were prepared by embedding the powder in L. R. White acrylic resin (hard) and sectioning on an ultramicrotome. The holey carbon film and the thin sections (~80 nm) were supported on 300 mesh copper grids.

Temperature-programmed cyclohexylamine desorption (CHA-TPD) spectra were recorded on a Cahn TG system 121 analyzer. Samples (~30 mg) were transferred directly out of the cyclohexylamine vapor to the thermobalance, and they were kept at 150 °C for 2 h. Desorption thermograms were recorded at a heating rate of 10 °C/min under nitrogen flow. The mass loss between 200 and 420 °C was used to determine the acid content of the samples (in mmoles CHA g^{-1} adsorbent).

Results and Discussion

As a member of the trioctahedral subgroup of 2:1 phyllosilicates, saponite contains primarily Mg^{2+} cations in each of the six octahedral positions of the $O_{20}(OH)_4$ unit cell, and a mixture of Si^{4+} and Al^{3+} ions in the eight tetrahedral positions of the cell. Consequently, the layer charge density is determined primarily by the Si/Al ratio in the tetrahedral sheet, and the layer charge is balanced by exchangeable cations in the gallery region between the 2:1 layers. Naturally occurring saponites usually have Fe^{2+}, Fe^{3+}, Mn^{2+}, and other transition metal ions substituting for Mg^{2+}, making them unattractive for catalytic applications. However, the mineral may be readily prepared by hydrothermal treatment of a slurry containing stoichiometric amounts of silica and either salts or hydroxides or oxides of Al and Mg together with a source for the interlayer cation.[17,18] The synthesis of saponites have been reported at temperatures below 100 °C either by using dilute solutions containing $AlCl_3$, $MgCl_2$, and $Si(OH)_4$ with reaction times of about 10 weeks,[19,20] or by coprecipitating sodium silicate and sodium aluminate with hydrochloric acid followed by a 45-day magnesium acetate treatment.[21] Most literature procedures for saponite synthesis, however, involve temperatures ranging from 200 to 450 °C and pressures between autogenous water pressure and 1500 bar.

In the present work we prepared three saponite compositions by hydrothermal treatment at 175−200 °C of reaction mixtures prepared from sodium metasilicate, magnesium nitrate and sodium aluminate for periods of about 20 h.[12] The reaction stoichiometries were targeted at unit cell compositions of $Na_x[Mg_6](Si_{8-x}Al_x)O_{20}(OH)_4 \cdot nH_2O$ with $x = 1.2$, 1.5, and 1.7. These charge densities were selected so that sufficient quaternary ammonium ions (denoted Q^+) and a neutral alkylamine cosurfactant could be subsequently incorporated into the galleries for PCH formation (see below). The resulting reaction products were designated SAP-1.2, -1.5, and -1.7, respectively.

Table 1 provides the Si/Al ratios of the synthetic saponite products as determined by chemical analysis and ^{29}Si MAS NMR spectroscopy. Included in the table are the experimentally determined cation exchange capacities (CEC). Table 1 also reports the corresponding unit cell formulas based on the chemical analyses.

(13) Booij, E.; Kloprogge, J. T.; VanVeen, J. A. R. *Clays Clay Miner.* **1996**, *44*, 774.
(14) Casal, B.; Merino, J.; RuizHitzky, E.; Gutierrez, E.; Alvarez, A. *Clay Miner.* **1997**, *32*, 41.
(15) Raimondo, M.; DeStefanis, A.; Perez, G.; Tomlinson, A. A. G. *Appl. Catal. A-Gen.* **1998**, *171*, 85.
(16) Sing, K. S. W.; Everett, D. H.; Haul, R. A. W.; Moscou, L.; Pierrotti, R. A.; Rouquerol, J.; Siemieniewska, T. *Pure Appl. Chem.* **1985,** *57*, 603.
(17) Harward, M. E.; Brindley, G. W. *Clays Clay Miner.* **1965**, *6*, 209.
(18) Kloprogge, J. T.; Breukelaar, J.; Jansen, J. B. H.; Geus, J. W. *Clays Clay Miner.* **1993**, *41*, 103.
(19) Decarreau, A. *Sci. Geol.* **1983**, *74*, 1.
(20) Farmer, V. C.; Krishnamurti, G. S. R.; Huang, P. M. *Clays Clay Miner.* **1991**, *39*, 561.
(21) Brat, S.; Rajan, N. S. S. *Indian J. Chem.* **1981**, *20A*, 311.

Table 1. Si/Al Ratios, Cation Exchange Capacities and Unit Cell Formulas for Synthetic Saponite Clays

	Si/Al				
sample	theor[a]	^{29}Si NMR spectroscopy	elemt. analysis	CEC (mequiv/100 g)	unit cell formulas[b]
SAP1.2	5.67	6.43	6.62	90	$Na_{1.11}Mg_{6.1}Al_{1.05}Si_{6.95}O_{20}(OH)_4$
SAP1.5	4.34	5.22	5.29	104	$Na_{1.33}Mg_{6.05}Al_{1.28}Si_{6.77}O_{20}(OH)_4$
SAP1.7	3.57	4.28	4.50	112	$Na_{1.48}Mg_{5.97}Al_{1.45}Si_{6.53}O_{20}(OH)_4$

[a] The Si/Al ratio of the initial gel prior to hydrothermal crystallization. [b] The unit cell formulas were found by elemental analysis.

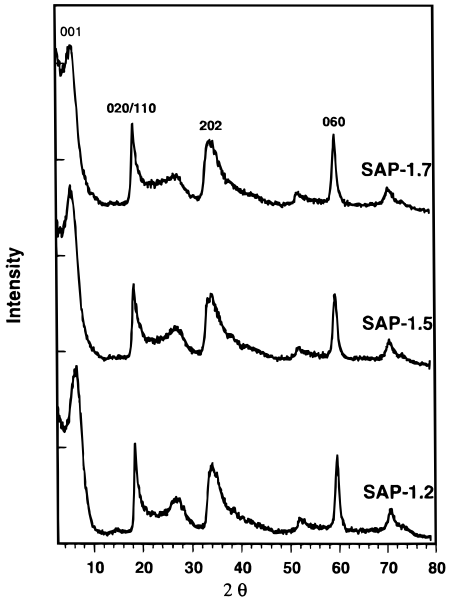

Figure 1. XRD Patterns of synthetic saponites.

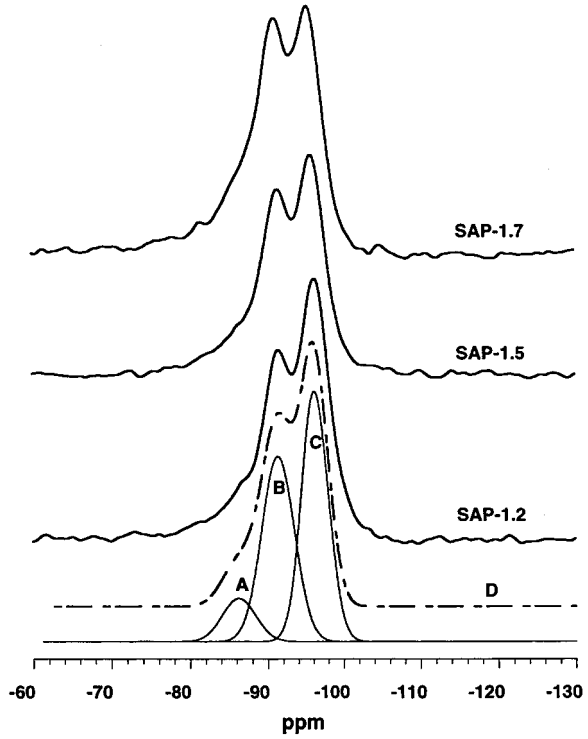

Figure 2. ^{29}Si MAS NMR spectra of synthetic saponites. The spectral components of the SAP-1.2 pattern (curves A, B, and C) were obtained by deconvolution of the observed spectrum. Curve D represents the sum of the components.

Figures 1 and 2 illustrate the X-ray diffraction patterns and ^{29}Si MAS NMR spectra, respectively, for the reaction products.

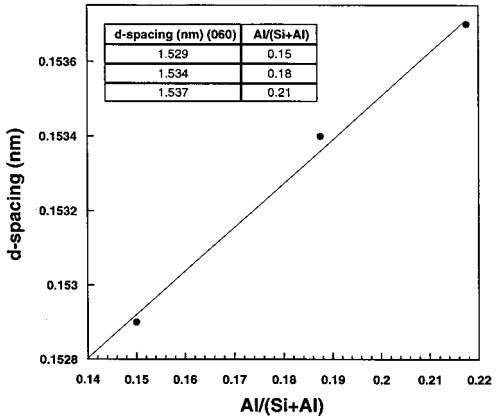

Figure 3. Dependence of the (060) spacing on the aluminum content of the tetrahedral layer of synthetic saponites.

All of the reaction products have a basal spacing of 12.5 Å and clearly exhibit the *hkl* reflections expected for a trioctahedral clay mineral (Figure 1).[18,19] Also, as shown by the plot of the basal spacing for the 060 reflection in Figure 3, the *b* lattice parameter increases in proportion to the aluminum content in accord with Vegard's Law.[22] This result verifies the incorporation of increasing amounts of aluminum into the layers with increasing aluminum content of the reaction gel.

The ^{29}Si MAS NMR spectra shown in Figure 2 also verify the structural composition of the saponite layers. Each sample exhibits two peaks at −95.8 and −90.5 ppm (Figure 2, curves C and B, respectively) and a shoulder at −86.1 ppm (Figure 2, curve A), which are assigned, in accord with previous NMR assignments,[23] to SiO_4 tetrahedra in $Q^3(0Al)$, $Q^3(1Al)$, and $Q^3(2Al)$, respectively. In this assignment scheme, the SiO_4 tetrahedra are linked to three adjacent tetrahedra containing one, two, or three aluminum centers. Increasing the amount of aluminum clearly results in an increase in the intensity of the $Q^3(1Al)$ resonance and, to a lesser extent, that of the $Q^3(2Al)$ signal, as well. The deconvolution of the ^{29}Si MAS NMR spectra allows for a quantitative assessment of the fraction of tetrahedral sites occupied by aluminum and, therefore, the determination of the Si/Al ratios through the relationship

$$\mathrm{Si/Al} = 3/\sum_{i=1}^{3} i\, \mathrm{I}_i$$

where *I* is the normalized intensities of the SiO_4 centers linked to *i* adjacent AlO_4 centers ($i = 1, 2, 3$).[23] The Si/

(22) Grauby, O.; Petit, S.; Decarreau, A.; Baronnet, A. *Eur. J. Mineral.* **1994**, *6*, 99.

(23) Lipsicas, M.; Raythatha, R. H.; Pinnavaia, T. J.; Johnson, I. D.; Giese, R. F.; Constanzo, P. M.; Roberts, J.-L. *Nature* **1984**, *309*, 604.

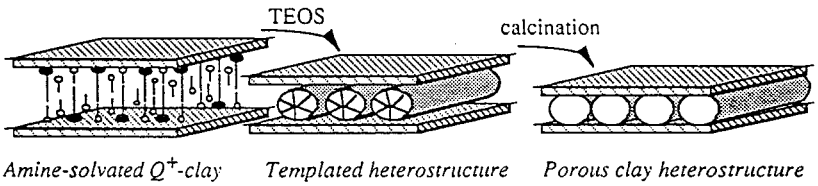

Figure 4. Schematic representation of porous clay heterostructure (PCH) formation through surfactant-directed assembly of open framework silica in the galleries of a layered silicate co-intercalated by a quaternary ammonium ion and a neutral amine cosurfactant.

Table 2. Properties of Q^+ and PCH Intercalates of Synthetic Saponites and Fluorohectorite

	d spacing (Å)					
sample	Q^+-saponite	PCH as-synthesized	PCH calcined	BET surface area[a] (m^2g^{-1})	pore volume[a] (cm^3g^{-1})	acidity (mmol CHA g^{-1})
SAP1.2-PCH	20.5	34.5	32.9	921	0.44	0.64
SAP1.5-PCH	24.2	35.9	34.2	877	0.42	0.73
SAP1.7-PCH	25.8	37.1	35.3	797	0.38	0.77
FH-PCH	27.0	38.0	32.0	700	0.35	0.10

[a] The surfaces areas and pore volumes are for the calcined forms of the PCH derivatives.

Al ratios determined by NMR are in good agreement with those found through elemental analyses (Table 1).

On the basis of the analytical results in Table 1, the layered structure tends to favor a higher Si/Al ratio than the ratio initially present in the gel prior to crystallization, and the deviations from the initial gel compositions increase with increasing layer charge density. Also, we note that the CEC values, which were determined by the exchange of sodium ions in the gallery by ammonium ions, increase in proportion to the aluminum content of the layers, as expected. However, the experimentally observed CEC values represent only ~70% of the values expected on the basis of the unit cell formulas in Table 1. It appears that sodium ion binding is preferred over ammonium ions under the conditions used in the exchange reaction, and this aspect of the exchange properties will require future investigation. Taken together, the above XRD, NMR, and analytical results clearly indicate that the synthetic saponite clays are very well crystallized and have compositions very near those targeted in the initial reaction stoichiometry.

All three saponites were used to assemble porous clay heterostructures that were denoted SAP1.2-, SAP1.5-, and SAP1.7-PCH, respectively. The process used to assemble the intragallery mesostructure, which is illustrated schematically in Figure 4, was analogous to the one previously reported for the preparation of PCH derivatives of fluorohectorite (FH-PCH).[9]

The basal spacings for the as-synthesized and calcined forms of the SAP-PCH derivatives (Table 2), as well as for the initial quaternary ammonium saponite precursors, increase with increasing aluminum content of the layers. The quaternary ammonium ions adopt paraffin-type arrangements in the interlayer space with chains radiating away from the clay surface.[24] As the layer charge density increases with increasing aluminum content, the onium ion orientation in the gallery becomes more vertical, resulting in an expansion of the gallery height. The increase in gallery height is accompanied by an increase in TEOS loading and, consequently in the amount of mesostructured silica in the gallery region of the final PCH. For instance, the gallery silica content per $O_{20}(OH)_4$ unit cell of the calcined product increases from 13.7 for SAP1.2-PCH to 15.7 mol for SAP1.7-PCH.

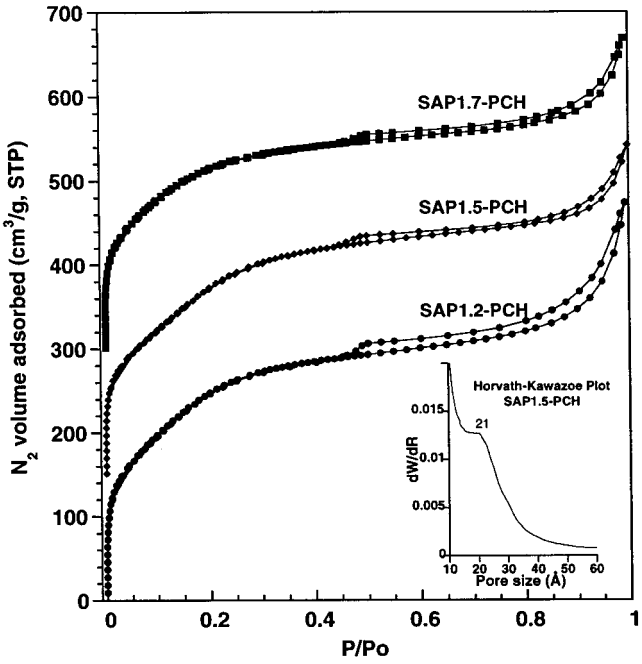

Figure 5. N_2 adsorption/desorption isotherms for porous clay heterostructures derived from synthetic saponites. The isotherms for SAP1.5 and SAP1.7-PCH are vertically displaced by 150 and 300 cm^3 g^{-1}, respectively. Insert: Horvath−Kawazoe pore size distribution curve. d*W*/d*R* is the derivative of the normalized adsorbate (N_2) volume adsorbed with respect to the pore diameter of the adsorbent in units of cm^3 g^{-1} $Å^{-1}$.

SAP-PCH derivatives exhibit specific surface areas and pore volumes that are even larger than those obtained for FH-PCH assembled from the same surfactant/cosurfactant system (Table 2).[9] Also, whereas FH-PCH begins to undergo defluorination above 350 °C and structural decomposition above ~550 °C, the SAP-PCH derivatives retain structural integrity even when calcined at 750 °C. As shown in Figure 5, the SAP-PCH products exhibit type IV adsorption isotherms. The near-linear uptake of nitrogen in the knee region corresponding to the partial pressure range 0.05−0.25 is indicative of a supermicropore to small mesopore structure in the supermicropore to small mesopore region, ~15−25 Å.[25,26] The inset to Figure 5 provides a typical pore size distribution. The BET specific surface

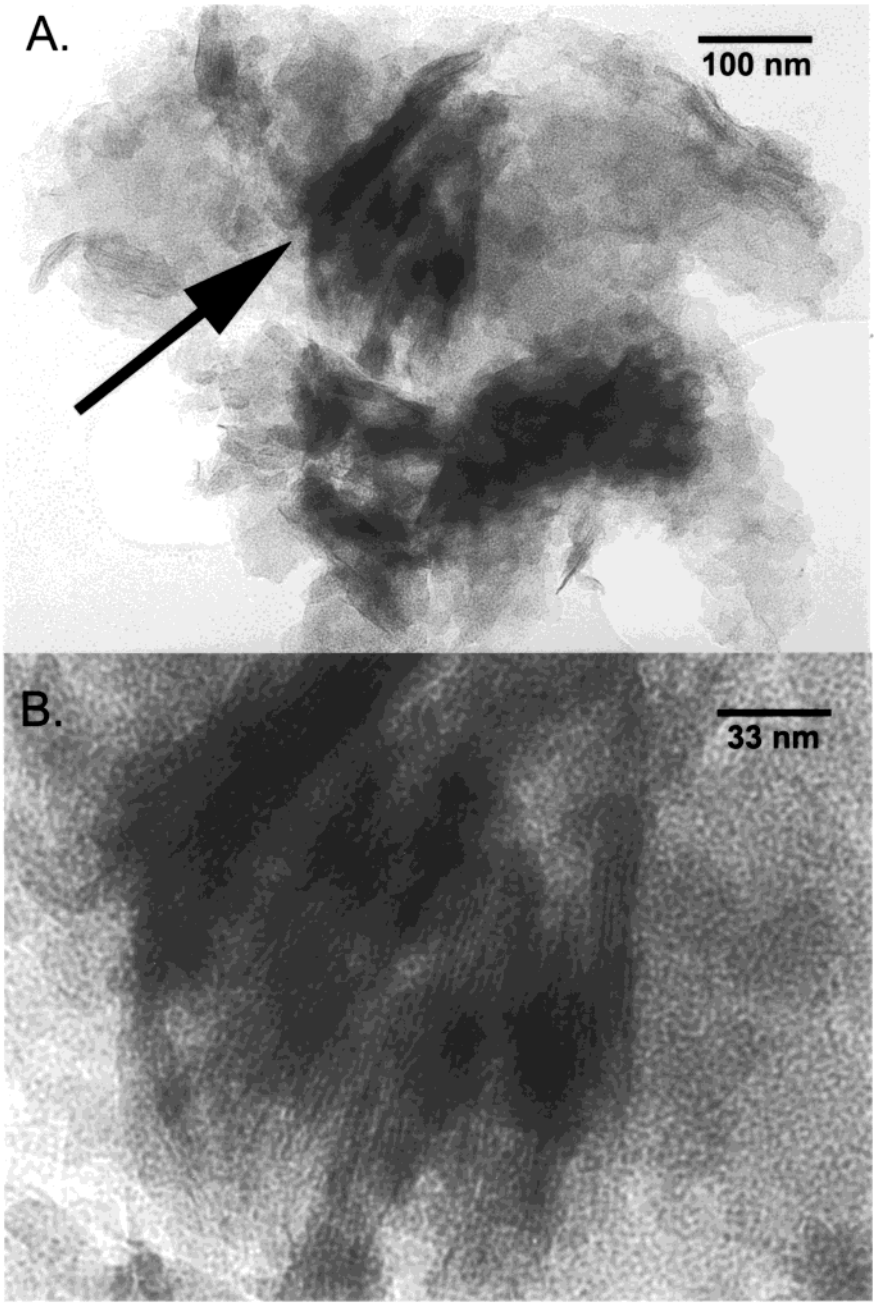

Figure 6. Representative TEM image of a calcined SAP1.5-PCH.

areas progressively decrease with increasing aluminum loading from 921 to 797 $m^2\ g^{-1}$ and the framework pore volumes decrease from 0.44 to 0.37 $cm^3\ g^{-1}$. This behavior is explained by the increased layer charge density, which results in an increase in the amount of mesostructured gallery silica.

Previous efforts to obtain TEM images of PCH materials have met with limited success.[9] Although the clay layers have been easily observed, resolving the intragallery pore structure has been more difficult due to the turbostratic nature of these materials. In the present work, direct imaging of the framework pores of SAP-PCH derivatives was achieved by thinning the samples along the *ab* plane through microtoming. Figure 6 is a typical TEM image of a SAP-PCH that has been suspended in ethanol and evaporated onto a holey carbon film. The low magnification image (see Figure 6A) shows that the larger particles consists of aggregated domains of several layers oriented in all directions, similar to the layer aggregation in the synthesized clay. The arrow in Figure 6A highlights the domains within the particle that are oriented with their *ab* planes parallel to the optic axis of the microscope. The lamellar phase is visible for this orientation of the domains. Other orientations of the *ab* planes reveal wormhole-like pores at the external surfaces of the clay plates. Tilting of the particle relative to the optic axis results in the reorientation of some of these domains parallel to the optic axis, again revealing the layered structure of these regions.

(24) Lagaly, G. *Solid State Ionics* **1986**, *22*, 43.
(25) Gregg, S. J.; Sing, K. S. W. *Adsorption, Surface Area and Porosity*, 2nd Ed.; Academic: London, 1983.
(26) Horvath, G.; Kawazoe, K. J. *J. Chem. Eng. Jpn.* **1983**, *16*, 470.

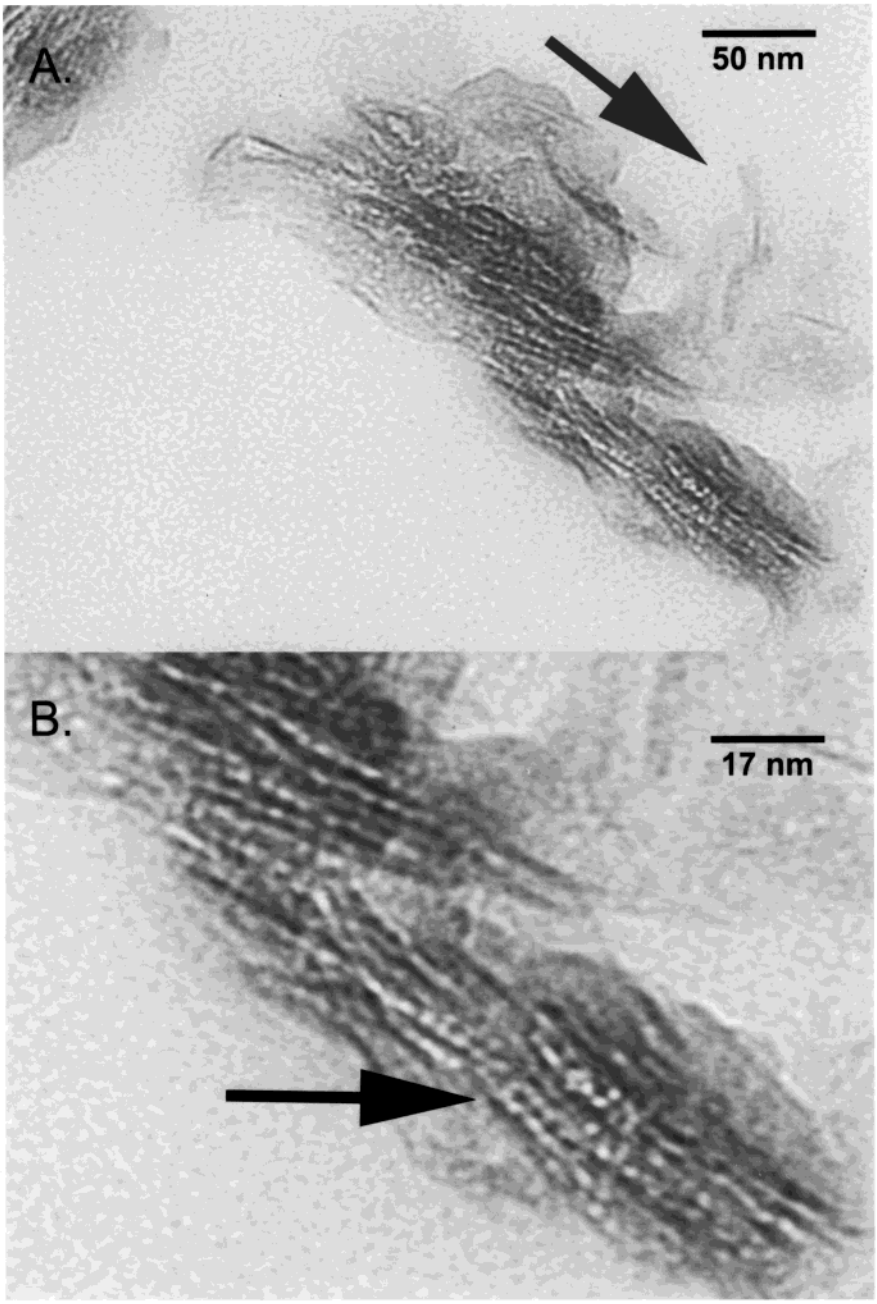

Figure 7. TEM of a thin-sectioned SAP1.5-PCH.

Figure 6B provides a higher magnification image of the oriented domains shown in Figure 6A. The lamellar phase and intragallery pore structure is clearly evident within this image. Due to the disorder of the pores within the gallery and the thickness of the particles, enhanced imaging of the intragallery pore structure is precluded. Improved imaging of the intragallery pore structure is possible, however, by sectioning the materials prior to imaging. Figure 7 shows typical TEM images of thin-sectioned a SAP-PCH in which the *ab* planes of the particle domain are oriented parallel to the optic axis. In the image provided in Figure 7A, the clay layers are discernible as solid dark lines and the pores appear in lighter contrast between the layers. The arrow in Figure 7A points to a small domain of three layers of SAP-PCH in which only the middle clay layer and the two adjacent gallery pore structures are clearly evident. The two outer clay layers are barely visible in this image.

Figure 7B is a higher magnification image of the intragallery pore structure. The pores within a gallery have a uniform size (arrow), as do the clay layers. The framework pore orientation is not persistent, however, indicating a significant degree of disorder within the gallery. A disorder wormhole-like pore structure in the *ab* plane is suggested by the changes in contrast levels between the layers.

The SAP-PCH materials reported here represent heterostructures comprising the smectite clay host and a mesostructured silica phase within the galleries of the host. The lattice substitution of silicon by aluminum in the clay layer and the replacement of the initial gallery ions (Na^+) by surfactant cations and subsequently by protons upon calcination, generate significant Brönsted

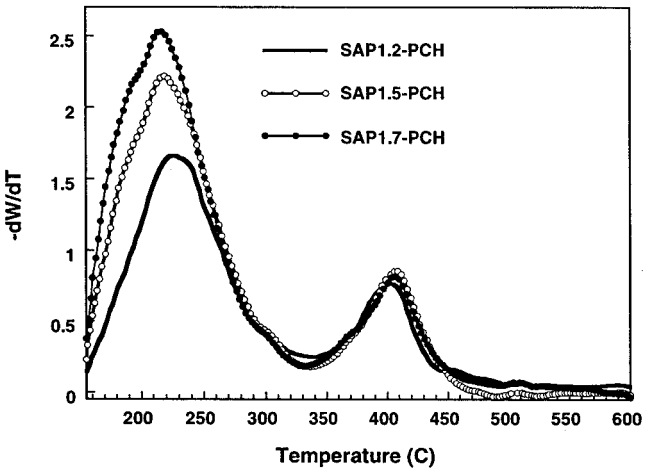

Figure 8. Profiles for the thermal desorption of cyclohexylamine from SAP-PCH samples. d*W*/d*T* is the differential weight with respect to temperature in units of g/°C.

acidity within the mesostructured galleries. The acid content of the SAP-PCH derivatives was determined using thermally programmed desorption of cyclohexylamine[27] (CHA-TPD). After being exposed to CHA vapor, the samples were heated at 150 °C for 2 h to remove the physically adsorbed amine.

As shown in Figure 8, the SAP-PCH materials exhibit two types of acidic sites. The intensity of the first desorption peak at 230 °C is directly correlated with the Si/Al ratio or the clay layers. This weaker acid site most likely is associated with the internal gallery surfaces of the PCH. The stronger acid site represented by the desorption peak near 410 °C is independent of the layer chemical composition and may related to sites at the external surfaces of the heterostructure. The weight loss of CHA between 200 and 420 °C was used to quantify the acidity, assuming that each base molecule interacts with one acid site. As expected, the number of acid sites increases due to an increase in the number of intragallery acid sites with increasing aluminum loading (Table 2).

(27) Breen, C. *Clay Miner.* **1991**, *26*, 487.

Conclusion

Synthetic saponite clays with layer charge densities above ~1.0 e^- units per $O_{20}(OH)_4$ unit cell are well-suited hosts for the intragallery, surfactant-directed assembly of mesostructured silica. The resulting porous clay heterostructures exhibit substantially higher acidity (0.64−0.77 mmol g^{-1}) than pillared clays (~0.24 mmol g^{-1}).[1−3] This feature of their chemistry, together with their unique pore structure in the supermicropore to small mesopore range and thermal stability to at least 750 °C should make them promising acid catalysts for organic chemical conversions, including gas oil cracking. Future work will focus on the catalytic properties of these materials.

Acknowledgment. The support of this research through NSF CRG grant CHE-9903706 and NIEHS grant ES04911D is gratefully acknowledged.

CM0002618